JCTC Journal of Chemical Theory and Computation

Article

pubs.acs.org/JCTC

Constant-pH MD Simulations of an Oleic Acid Bilayer

Diogo Vila-Viçosa,[†] Vitor H. Teixeira,[†] António M. Baptista,[‡] and Miguel Machuqueiro*[,†]

[†]Centro de Química e Bioquímica and Departamento de Química e Bioquímica, Faculdade de Ciências, Universidade de Lisboa, Edifício C8 Campo Grande, 1749-016 Lisboa, Portugal

[‡]Instituto de Tecnologia Química e Biológica, Universidade Nova de Lisboa, Av. da República, 2780-157 Oeiras, Portugal

Supporting Information

ABSTRACT: Oleic acid is a simple molecule with an aliphatic chain and a carboxylic group whose ionization and, consequently, intermolecular interactions are strongly dependent on the solution pH. The titration curve of these molecules was already obtained using different experimental methods, which have shown the lipid bilayer assemblies to be stable between pH 7.0 and 9.0. In this work, we take advantage of our recent implementations of periodic boundary conditions in Poisson−Boltzmann calculations and ionic strength treatment in simulations of charged lipid bilayers, and we studied the ionization dependent behavior of an oleic acid bilayer using a new extension of the stochastic titration constant-pH MD method. With this new approach, we obtained titration curves that are in good agreement with the experimental data. Also, we were able to estimate the slope of the titration curve from charge fluctuations, which is an important test of thermodynamic consistency for the sampling in a constant-pH MD method. The simulations were performed for ionizations up to 50%, because an experimentally observed macroscopic transition to micelles occurs above this value. As previously seen for a binary mixture of a zwitterionic and an anionic lipid, we were able to reproduce experimental results with simulation boxes usually far from neutrality. This observation further supports the idea that a charged membrane strongly influences the ion distribution in its vicinity and that neutrality is achieved significantly far from the bilayer surface. The good results obtained with this extension of the stochastic titration constant-pH MD method strongly supports its usefulness to sample the coupling between configuration and protonation in these types of biophysical systems. This method stands now as a powerful tool to study more realistic lipid bilayers where pH can influence both the lipids and the solutes interacting with them.

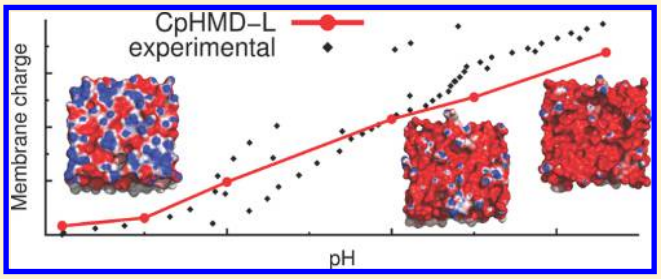

1. INTRODUCTION

Lipids are one of the most important macromolecules in living systems. They have crucial roles as structural components of biological membranes, in energy storing, and as signaling molecules.[1] Many of the biologically relevant lipids are anionic and their ionization may depend on the solution pH.[2] Hence, pH affects many biological processes involving lipid protonation such as membrane fusion, cholesterol domain formation, drug−liposome interactions, and membrane phase transitions.[3]

The study of the properties of lipidic structures poses many different challenges when compared to the most studied macromolecule—proteins. Lipid conformations are intrinsically dependent on their macromolecular assemblies, and thus they can not be studied individually. Both experimental and theoretical methods need adjustment to study these molecules in their biologically relevant environment. In particular, molecular modeling techniques require the use of periodic boundary conditions (PBC) to mimic an infinite bilayer.[4] Also, the ionic strength local effects have to be accounted when the system size is as small as a standard simulation box.[5] Nevertheless, it is now possible to model, at atomic level, large and complex lipidic systems using molecular mechanics/dynamics (MM/MD) simulations with explicit solvent.[6] To increase the realism of these models, it is necessary to add anionic lipids whose ionization depends on the solution pH. However, MM/MD simulations deal with pH in a limited way, simply by setting a fixed protonation state for each titrable group. On the other hand, there are simple models that can estimate the protonation state for a rigid structure, such as those based on the Poisson−Boltzmann (PB) equation[7−12] and on a Monte Carlo (MC) sampling.[13−15] The limitations of the previous methods gave rise to the so-called constant-pH MD methods (CpHMD)[16−45] that, in some cases, take advantage of the complementarity between MM/MD and PB/MC methods. In these methods, the titrable groups are allowed to change their protonation state along the simulation time. Thus, it is possible to study the protonation/conformation coupling in the system of interest by setting a pH value and running a simulation with pH as an external parameter such as temperature or pressure. These methods are often used with proteins and it is nowadays possible to perform complete titrations of these molecules.[17,21−25,27−35,38,39,41−44] However, the application of such methods to lipid bilayers poses two main challenges: on the one hand, the correct description of the PBC in the PB calculations[4] (in the methods that use them)

Received: February 2, 2015
Published: April 10, 2015

DOI: 10.1021/acs.jctc.5b00095
J. Chem. Theory Comput. 2015, 11, 2367−2376

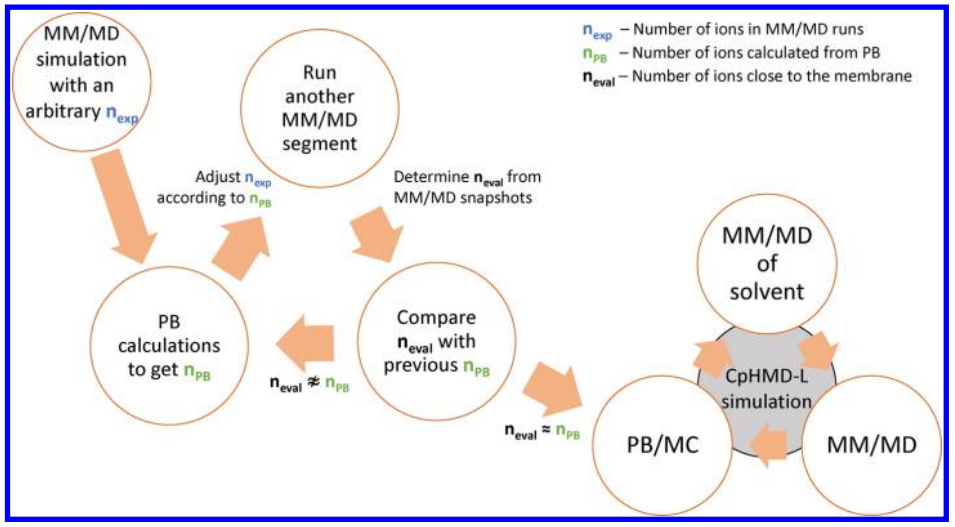

Figure 1. Workflow to calculate the final number of explicit ions obtained from the self-consistent procedure (adapted from ref 5).

and, on the other hand, the treatment of the ionic strength effect close to charged lipid bilayers.[5] Recently, a constant-pH MD approach was applied to oleic acid aggregates using a coarse-grained model,[37] treating the protonation of the titrable residues as a continuous variable[22,46−48] analogously to λ-dynamics.[49] Using a similar theoretical basis, Shen and co-workers studied the pH-dependent self-assembly of lauric acid at atomistic level.[50]

The use of PBC is well established in biomolecular models and can be applied in the electrostatic calculations needed for the stochastic titration constant-pH MD method.[4] However, the treatment of ionic strength is not trivial, and different approaches have been proposed. Charge-leveling has been used to preserve the electroneutrality in the context of a constant-pH MD method[36] and applied to several dicarboxylic acids. However, electroneutrality may not be appropriate in some systems. In particular, a charged lipid bilayer induces a local ion concentration that can be far from neutrality and very different from the bulk ionic strength.[5,9,51−58] In ref 5, we proposed a PB-based method to estimate the number of ions close to a lipid bilayer and tested this estimate in MD simulations of a 25% PA/PC lipid mixture.

In this work, we developed a new extension of the stochastic titration constant-pH MD method[18,24] to deal with lipid bilayers of oleic acid, taking advantage of the recent implementations of PBC in PB calculations[4] and ionic strength in membrane simulations.[5] Oleic acid is a simple molecule with a carboxylic group and a carbon chain of 18 carbons with one insaturation. The ionization of carboxylic acids and, consequently, their intermolecular interactions are strongly dependent on the solution pH. In particular, oleic acid can be present as either liposomes or micelles.[59−63] Moreover, the apparent pK_a value of oleic acid in these aggregated phases is somewhat ill-defined and difficult to estimate[59−62] and, depending on the used method, can vary between 7.5 at low concentrations inserted in a PC bilayer[64] and 9.85 in pure monolayers.[65] There are also three independent oleic acid titration experiments that report lipid bilayer assemblies between pH 7.0 and 9.0 (above this value a phase transition into micelles is observed).[59,60,62] Here, we performed several constant-pH MD simulations of a bilayer of oleic acid in order to study the pH-dependence of its structure. The total titration curve obtained for the bilayer was compared with the available experimental data measured for this macromolecular assembly.

2. METHODS

2.1. Stochastic Titration Constant-pH MD. The stochastic titration constant-pH MD method[18,24] works in a cycle with three main steps, with the loop running until the end of the desired simulation time (Figure 1 and Figure S1 in Supporting Information). In the Poisson−Boltzmann/Monte Carlo (PB/MC) step, the protonation states of the solute are sampled using MC calculations[13−15] with free energies obtained from PB calculations.[7−12] The final protonation states are then assigned to the solute in the Molecular Mechanics/Molecular Dynamics (MM/MD) steps. The second block consists of a short MM/MD simulation (during a time interval τ_{rlx}) with the solute frozen and in the NVT ensemble with the objective of relaxing the water molecules to the new protonation states. The last step of the cycle is a production MM/MD simulation during a time interval τ_{prt} with all system unfrozen.

In a bilayer environment, the correct description of the periodicity of the system along the membrane plane is crucial. In the MD steps, the periodic boundary conditions (PBC) corrections are readily available in most software packages. However, for PB calculations, the use of 2D-PBC presents a few new challenges.[4] We have addressed the inclusion of 2D-PBC in the PB calculations to study the protonation of a DMPC molecule using a linear response approximation.[4] The same approach was adopted in the current CpHMD implementation for lipidic systems (CpHMD-L).

The treatment of the ionic strength effect on a charged lipid bilayer is not trivial. In particular, it has been suggested by several authors that the use of full neutralization is not the most adequate approach to deal with this problem.[9,51−58] To simulate a neutral system, one would need to use a very large simulation box (in z direction), which would be too time-consuming. Recently, we have developed a method to deal with ionic strength in charged systems.[5] This method uses a PB model to estimate the amount of counterions and co-ions near a charged membrane. The number of ions is computed in the region between the membrane surface and the cutoff value used in the treatment of long-range electrostatics (1.4 nm; see section "MM/MD settings"). The region beyond the cutoff value is kept relatively small, avoiding significant trapping of

DOI: 10.1021/acs.jctc.5b00095
J. Chem. Theory Comput. 2015, 11, 2367−2376

ions. The PB-estimate of the total amount of ions in this region (n_{PB}) is given by

$$n_{PB} = \int_C \rho(\mathbf{r})\mathrm{d}v \approx VN_A I \sum_{i=1}^{M} \mathrm{e}^{-ze\phi_i/k_B T} \quad (1)$$

where the region of interest C is discretized into a set of M small cells, each with volume V and approximately constant electrostatic potential, $\rho(\mathbf{r})$ is the number density of an ion at position $\mathbf{r}$ with charge z, ϕ_i is the electrostatic potential in cell i, ρ_0 is the bulk number density, e is the elementary charge, k_B is the Boltzmann constant, I is the ionic strength, and T is the absolute temperature. The number of cations, $n_{PB}(Na^+)$, and of anions, $n_{PB}(Cl^-)$, is calculated for each of a set of configurations from a MD simulation. The median, which is robust to outliers, of these calculated values is then used as an estimation for the next MD simulation of the same system.

The final numbers of explicit ions, $n_{exp}(Na^+)$ and $n_{exp}(Cl^-)$, are determined as follows (Figure 1). A first MM/MD simulation is performed by setting n_{exp} to any number between 0 and a sufficient amount to neutralize the system (the initial guess does not affect the final converged result). After this, the first set of n_{PB} values is calculated from eq 1, and the number of ions in the simulation (n_{exp}) is adjusted accordingly. We then determine the average numbers of explicit ions that are closer than 1.4 nm to the membrane in the new simulation, $n_{eval}(Na^+)$ and $n_{eval}(Cl^-)$. After the calculation of both n_{PB} and n_{eval} the two pairs of values are compared and, if necessary, n_{exp} is adjusted for a new MD simulation. This process continues iteratively until $n_{eval} \approx n_{PB}$; that is, the process becomes self-consistent (usually after 2 or 3 iterations).

In this work, we take advantage of these two recent developments[4,5] regarding the PBC in PB calculations and the explicit ions estimation in charged bilayer systems, and we implement them in an extension to the stochastic titration constant-pH MD method (CpHMD-L).

2.2. Charge Fluctuations and Slope of the Titration Curve. All protonation states of a system with multiple titration groups are in equilibrium with each other and the solution. Which means that, at a given pH value, the total charge of the system (in our case, a membrane) is not a constant, rather fluctuating around an average value (see Figure 4a below). These fluctuations are related with the slope of the titration curve through:[66]

$$\frac{\partial \bar{Z}}{\partial \mathrm{pH}} = -\ln(10)\sigma^2 \quad (2)$$

where $\bar{Z}$ and σ are, respectively, the average and the standard deviation of the membrane charge at a given pH value. This is a particular case of the general equation holding for the number of bound molecules of a ligand, relating its fluctuation with the derivative of its average with respect to ligand activity,[67] which is itself a particular case of the analogous relation for the number of particles in a grand canonical ensemble.[68]

The above relation can be used to test if the CpHMD-L method is able to correctly sample the charge fluctuations of a membrane. This was done here by comparing two cubic splines computed from the simulation data using slopes taken either from the MD simulations (through eq 2) or directly estimated from the average protonations using the Davis−Dowden method for monotone data.[69] The two splines thus obtained should be very similar if our constant-pH MD method is thermodynamically consistent, as it was found indeed to be the case (see Figure 4b and the accompanying text).

2.3. Constant-pH MD Settings. The CpHMD-L simulations were performed using three ionic strength values (0.1, 0.3, and 0.5 M). The values above 0.1 were chosen in order to increase the membrane stability at higher pH values (see Results and Discussion). It should also be noted that the ionic strength values were not reported in the titration experiments.[59,60,62] All simulations were done in triplicate for 100 ns each (Table 1). The number of ions in each simulation depends on the ionic strength and on the membrane ionization. All systems were pre-equilibrated using standard MM/MD simulations with ionization from 0% to 50%. For these equilibrations, we used the self-consistent algorithm (Figure 1) previously explained. The self-consistency between n_{eval} and n_{PB} values for all CpHMD-L simulations was confirmed *a posteriori* (see section "Estimation of the Number of Ions and System Equilibration").

Table 1. Summary of the Simulations Performed in This Work[a]

I/M	pH	n_{exp} (Na^+)	n_{exp} (Cl^-)
0.1	6.00	2	2
0.1	6.50	2	2
0.1	7.00	3	2
0.1	7.25	4	2
0.3	6.00	5	5
0.3	6.50	6	5
0.3	7.00	10	8
0.3	8.00	14	8
0.5	6.00	9	9
0.5	6.50	10	9
0.5	7.00	15	10
0.5	8.00	20	12
0.5	8.50	26	12
0.5	9.30	34	12

[a]One hundred oleic acid molecules were used in all simulations.

We also tested several τ_{prt} values, 2, 20, and 50 ps, starting from structures equilibrated at 20, 30, 40, and 50% of ionization, from one structure with high area per lipid (A_l) and another with low A_l. These tests were necessary because the best protonation frequency for lipid bilayers may differ from the one used in protein systems (usually 2 ps). The best values are always a compromise between computational speed and the convergence of protonation and configuration, which are coupled. The τ_{rlx} value, on the other hand, was the same as for proteins (0.2 ps). Because all these simulations were performed at pH 8.0 and I = 0.5 M, in principle, they should converge to the same values (of both A_l and ionization—see Results and Discussion).

2.4. MM/MD Settings. MM/MD simulations were done using the GROMOS 54a7 force field[70] and a modified version[18,24] of GROMACS distribution (version 4.0.7[71,72]). The MM parameters for the hydrocarbon chain of oleic acid were taken from the POPC molecule (in ref 73) and for the carboxylic group were taken from the glutamate side chain present in GROMOS 54a7 force field.[70] All simulations were performed using Na^+ as a cation, even though we have shown that similar results can be obtained with K^+.[5] Cl^- was used as anion in all simulations. The membrane was solvated in a tetragonal box with SPC water molecules,[74] with the membrane

DOI: 10.1021/acs.jctc.5b00095
J. Chem. Theory Comput. 2015, 11, 2367−2376

surface oriented parallel to the *xy* plane. All bond lengths were constrained using the parallel version of the LINCS algorithm for lipids[75] and the SETTLE algorithm[76] for water. All NPT simulations were done using the v-rescale thermostat[77] at 298 K with separate couplings for the solute and solvent (including ions) with a relaxation time of 0.1 ps. A semi-isotropic Berendsen[78] pressure couple was used to maintain the pressure constant at 1 bar with a compressibility of 4.5×10^{-5} bar^{-1} and a relaxation time of 5.0 ps. In CpHMD-L simulations, the solvent relaxation steps were performed in the NVT ensemble. An integration step of 2 fs was used in the MD equations of motion. Nonbonded interactions were treated with a twin-range method, using group-based cutoffs of 0.8 and 1.4 nm, updated every five steps. Long-range electrostatics were corrected with a generalized reaction field (GRF),[24,79] using a dielectric constant of 54.0, which has been shown to minimize artifacts due to electrostatic interactions truncation and their approximation by an infinite dielectric continuum.[80]

The minimization procedure consisted of three sequential steps: starting with the steepest descent algorithm (unconstrained), followed by 10 000 steps using the low-memory Broyden−Fletcher−Goldfarb−Shanno integrator (unconstrained), and ended with another step using the steepest descent algorithm (with all bonds constrained).

The same initialization procedure was applied to all systems and consisted of four steps. First, a 50 ps MD simulation was done with all heavy atoms harmonically restrained with a force constant of 1000 kJ mol^{-1} nm^{-2}. In the three following steps of 100, 150, and 200 ps MD simulations, position restraints were applied differently for the carbon atom of the carboxylic group and remaining heavy atoms, with force constants of 1000, 100, and 10 kJ mol^{-1} nm^{-2} and of 100, 10, and 0 kJ mol^{-1} nm^{-2}, respectively.

2.5. PB/MC Settings for CpHMD-L Simulations. The PB calculations were done with the program DelPhi V5.1[81,82] using atomic radii and partial charges taken from GROMOS 54a7 force field.[70] The molecular surface of the membrane was defined by a probe of radius 0.14 nm, and the ion exclusion layer was 0.2 nm. In order to avoid discontinuities in the PBC surface (Delphi does not calculate the molecular surface taking PBC into account), we added a small portion (5% of the box side dimension) of the membrane atoms in the *x* and *y* directions.[4] PBC were explicitly applied along those two directions in the calculation of the potential. A convergence threshold value based on maximum change of potential of 0.01 $k_B T/e$ was used. All PB calculations in the CpHMD-L workflow were done in a cubic grid with 45 grid points (corresponding to a grid space of ~0.08 nm) and a two-step focusing,[83] where the focus grid was one-fourth of the coarser grid size. In the iteration convergence process of finite differences method, we used relaxation parameters for the nonlinear and linear forms of the PB equation with values of respectively 0.75 and 0.20. A cutoff of 1.6 nm was used to calculate the background and pairwise interactions (see ref 4 for more details). The pK_a values of the model compounds (carboxylic group) were taken from the pK_a value of acetic acid in solution (4.76).[84] The dielectric constant of the solvent was 80, and for the membrane, we used a value of 2.

The MC sampling was performed with the PETIT program[15] version 1.6 using an absolute temperature of 298 K. All runs were performed using 10^5 MC cycles, where one cycle consists of sequential state changes over all individual sites and pairs of sites with an interaction larger than 2 pH units.

2.6. PB Settings for Ion Estimation. The PB calculations performed for the ion estimation are similar to those described in the previous section. The focusing procedure was not used because we are interested in all grid points closer than 1.4 nm to the membrane. In the iteration convergence process of finite differences method, we used relaxation parameters for the nonlinear and linear forms of the PB equation with values of respectively 0.15 and 0.20. In these calculations, we used 450 configurations from each simulation. To estimate the number of ions (n_{PB}), the electrostatic potential is written to a new 3D grid with 50 points per side, the same size as the finite differences grid.[4] The number of ions were calculated according to eq 1.

2.7. Analysis. The last 90 ns of each simulation were used for analyses. Several tools from the GROMACS software package[71,72] were used. A_l was defined as the average *xy* area occupied by a lipid molecule. Deuterium order parameters were calculated taking in consideration a bug correction introduced in GROMACS 4.5.4.[85] All presented errors were computed using standard methods based on the autocorrelation function of the property measured to determine the number of independent blocks in the simulations.[86]

3. RESULTS AND DISCUSSION

3.1. Calibration of the τ_{prt} Parameter. The duration of the production MM/MD step in the constant-pH MD cycle (τ_{prt}) is an important variable in our constant-pH MD simulations, because a value too large may originate insufficient sampling of protonation states, and a value too small may increase the computational cost and destabilize the solute conformation/configuration (see below). Hence, we performed a set of simulations with three τ_{prt} values (2, 20, and 50 ps—see Methods for details). In these simulations, we checked the convergence of both A_l and ionization (Figure 2 and Figures S1 and S3 in Supporting Information). For τ_{prt} = 2 ps, the membrane became too unstable and disrupted in the first nanoseconds of simulation. This destabilization was probably caused by the large oscillations in the membrane charge. Despite the fact that this τ_{prt} value is usually used in simulations of proteins with the stochastic titration constant-pH MD

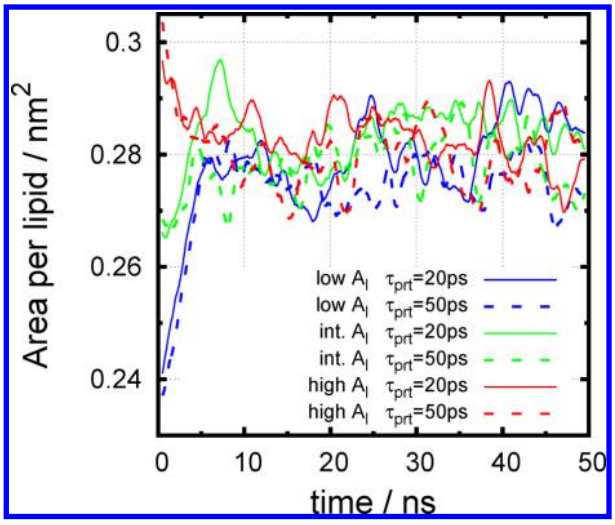

Figure 2. Time variation of area per lipid in simulations to calibrate the τ_{prt} parameter. Three groups of simulations are shown, starting from low, intermediate, and high A_l.

DOI: 10.1021/acs.jctc.5b00095
J. Chem. Theory Comput. 2015, 11, 2367−2376

method,[18,24] it might not be appropriate for a lipid bilayer. The fluctuations of the amino acid side chains are usually in a time scale much faster than lipid diffusion, therefore a larger τ_{prt} value is needed for the lipids to adapt to new protonation states. Not doing so can result in local instabilities and membrane disruption. For both τ_{prt} = 20 ps and τ_{prt} = 50 ps, all the simulations were structurally stable during 50 ns and both A_l and protonation converged rapidly (in less than 10 ns) to the same values (Figure 2 and Figures S2 and S3 in Supporting Information). Therefore, both τ_{prt} values were suitable to be used in the present work. We chose the τ_{prt} value of 20 ps mainly due to its more extensive sampling of protonation states and the consequent smaller chance of falling into kinetic traps during the simulations. A smaller τ_{prt} could better capture the protonation/configuration coupling in a lipid bilayer, which can be challenging for lipid molecules other than oleic acid.

3.2. Estimation of the Number of Ions and System Equilibration. Ionic strength is a macroscopic property that is very complex to modulate at a microscopic level. As explained in the Methods section, we used a methodology described in ref 5 to deal with the ionic strength effects in our systems. Hence, the number of ions in our simulations is not always the same, and it depends both on the ionic strength and on the average degree of ionization. It is possible to confirm the number of ions that should be present in a CpHMD-L simulation comparing the number of explicit ions that we introduced *a priori* (Table 1) with an estimation using the PB formalism.[5]

The number of ions was calculated by averaging the estimations with the PB-based approach from 450 structures taken from the last 90 ns of each simulation (Figure 3). The

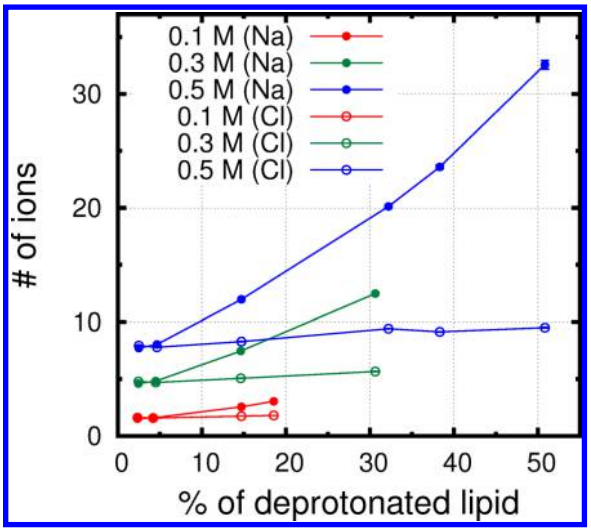

Figure 3. Number of counterions and co-ions in all CpHMD-L simulations at different membrane ionization values. Membrane ionization was obtained from the total titration curves (see Figure 4) below.

number of both sodium and chloride ions increases with ionic strength. Hence, at higher ionic strength values, there are more ions available to stabilize the repulsions between the headgroups leading to more stable membranes. Interestingly, despite our membrane being negatively charged, there are always chloride ions. The fact that the number of these ions does not change significantly with ionization, can be explained by two opposite effects. On the one hand, its concentration decreases near the membrane, due to the negative potential generated by the anionic lipids (see the ion concentration variation with the ionization in Figure S4 in Supporting Information). On the other hand, the A_l (see Figure 5), hence the volume where the number of ions is estimated, increases, thereby compensating the first effect.

Sodium ions, which in principle are the more important stabilizers of the negatively charged membranes, are also present in a small number (according to the ionic strength) when the membrane is almost neutral (see Figure S5 in Supporting Information for a representation of the PB-estimated electrostatic potential used to estimate the number of ions). This number increases with the bilayer ionization because the counterions are attracted to the more negative membrane.

3.3. Membrane Titration. The CpHMD-L simulations of an oleic acid bilayer allow us to follow the total membrane charge over time at different pH values (Figure 4a). In all simulations, this charge converges very fast (in the subnanosecond time scale) to an average value. In addition, the charge fluctuations around the average are significantly large (more than 15 charge units at high pH values), which emphasizes the need to use the CpHMD-L method with these systems rather than standard MM/MD simulations at constant protonation. As mentioned in the Methods section, the accuracy of these fluctuations can be checked by converting them into slopes of the titration curves and comparing the resulting cubic splines with those obtained with a standard method (Figure 4b). The very good agreement between the two cubic splines indicates that our method is correctly sampling not only the average protonation values (see below) but also the charge fluctuations.

The titration curve of oleic acid was computed by averaging the occupancy states of all oleic acid molecules over the last 90 ns of each simulation (Figure 4c). Our simulations were done using three ionic strength values (see Methods) and compared with different experimental results.[59,60,62] There are no abrupt changes in the titration curves, and there is a large shift between the titration region and the model compound pK_a value (4.76), as expected for such a highly anticooperative system.

Haines et al. have measured a potentiometric titration curve at room temperature from pH 12 to 6 of a dispersion of 50 mM oleic acid and 10 mM lauric acid.[59] More recently, Peterlin et al. obtained an equilibrium titration curve of a 9.9 mM pure oleic acid suspension at 298 K.[62] Despite the slight discrepancy at lower ionization (Figure 4c), there is consistency between these two independent measurements in the bilayer region. We observe good agreement between our titration curves and these experiments for all ionic strength values. In fact, our curves are not significantly shifted upon changes in the ionic strength. This observation may be related with two opposite effects of ionic strength on the protonation of lipids in our model. On the one hand, at a higher ionic strength, the interaction between the headgroups are weaker, leading to higher ionization and the consequent deviation of the titration curve to lower pH values. On the other hand, the same effect can approximate the headgroups (lowering the A_l) resulting in higher percentage of protonation and deviating the curve to higher pH values.

Cistola et al. have also measured a titration curve of pure oleic acid (80 mM) at 313 K following ^{13}C NMR chemical shifts.[60] This experimental curve is shifted to lower pH values compared to our results and the other experimental curves. These measurements were carried out at higher temperature, and thus it is expected that the average distance between the

DOI: 10.1021/acs.jctc.5b00095
J. Chem. Theory Comput. 2015, 11, 2367−2376

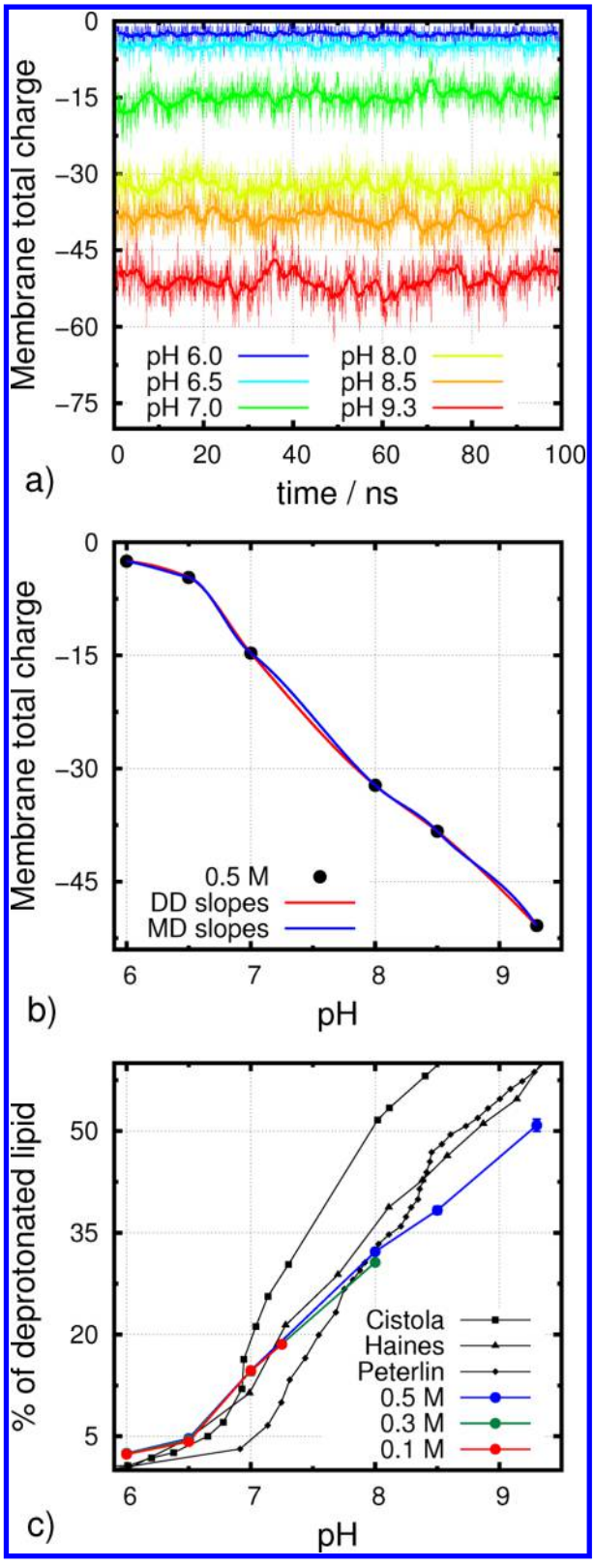

Figure 4. Titration of lipid bilayer. Membrane charge vs simulation time for one replicate per pH at I = 0.5 M (a). Simulated titration curves where the values are connected using cubic splines whose slopes are estimated using either eq 2 (MD) or the Davis-Dowden method (DD) (b). Simulated and experimental titration curves (c). All simulated titration curves were obtained in this work with the CpHMD-L simulations and for the experimental we used the data from Cistola et al.,[60] Haines et al.,[59] and Peterlin et al.[62]

headgroups and, consequently, the solvent exposure, are higher, favoring the ionized form of these groups.

The experimental titration curves were obtained for a wide range of pH values. However, we were only able to run our simulations at pH values up to 7.25, 8.00, and 9.30 using, respectively, I = 0.1, 0.3, and 0.5 M. Above these values, the membrane became unstable and disrupted due to the strong repulsions between the negatively charged headgroups. At lower ionic strength values, the number of counterions available are not sufficient to stabilize these repulsions even at lower ionizations. The membrane disruption at I = 0.5 M and pH 9.30 is in agreement with the experiments suggesting that above pH 9.0 (8.0 in ref 60 due to a higher temperature) a phase transition to micelles occurs. In fact, it is possible that the small deviation observed between our titration curve and the experiments[59,62] at higher ionizations can be explained by the coexistence of liposomes and micelles in the experimental dispersion. At lower ionization, a phase transition into oil droplets has been experimentally observed.[59] In our simulations, because all systems were built as bilayers, the oil droplet phase representation is characterized by tightly packed configurations with slow diffusion rates (see Section 3.4 and and Figures S10, S11, and S12 in Supporting Information).

The total system charge varies approximately between −2 (at low pH) and −25 (at high pH) (Figure 3), which results in several systems far from neutrality. In our work, we were able to reproduce the experimental titration curve with stable bilayers, further supporting the idea that such small and charged systems do not always need to be neutralized. These findings are in agreement with previous observations about neutrality only being achieved much farther away from a charged membrane.[5,9,51−58]

3.4. Membrane Structural Parameters. The area per lipid (A_l) is one of the most commonly used properties to describe the behavior of lipidic membranes and directly reflects their phase transitions. From our CpHMD-L simulations, we can follow the x and y dimensions of the simulation box at different pH/ionization values and calculate the A_l of the lipid bilayer (Figure 5). This property increases with pH in almost all simulated pH range. This is expected since the ionization of the carboxylic headgroups leads to higher electrostatic repulsions (Figure 6). Nevertheless, we observe two plateaus at pH 6.0−6.5 (∼3−5% of ionization) and at pH 8.0−8.5 (∼30−40%). In the first case, the lipid bilayer is in a very ordered gel phase (∼0.22 nm^2) with tightly packed lipid configurations (Figure 6, left panel). Only at slightly higher pH values (pH 7.00) it is possible to disrupt these very stable configurations and increase both ionization and A_l. The second plateau is probably related with the bilayer stability limits, because we observed that the bilayer becomes very unstable at pH 9.3, as pointed above.

As observed for the total titration curves, there is no significant influence of the ionic strength on the A_l. At lower ionic strength, the lipid bilayer gets disrupted at relatively low A_l values due to the lack of enough stabilizing counterions. There is a clear pH-dependent isothermal phase transition between a very ordered gel phase (pH 6.0−6.5) and a highly dynamic fluid phase (pH 9.3). At higher pH values, the lipid bilayer gets disrupted, probably because micelles became the most stable assembly, as shown in many experiments.[59,60,62] A detailed study of these micellar assemblies could not be accomplished with our systems construct and is out of the scope of this work.

DOI: 10.1021/acs.jctc.5b00095
J. Chem. Theory Comput. 2015, 11, 2367−2376

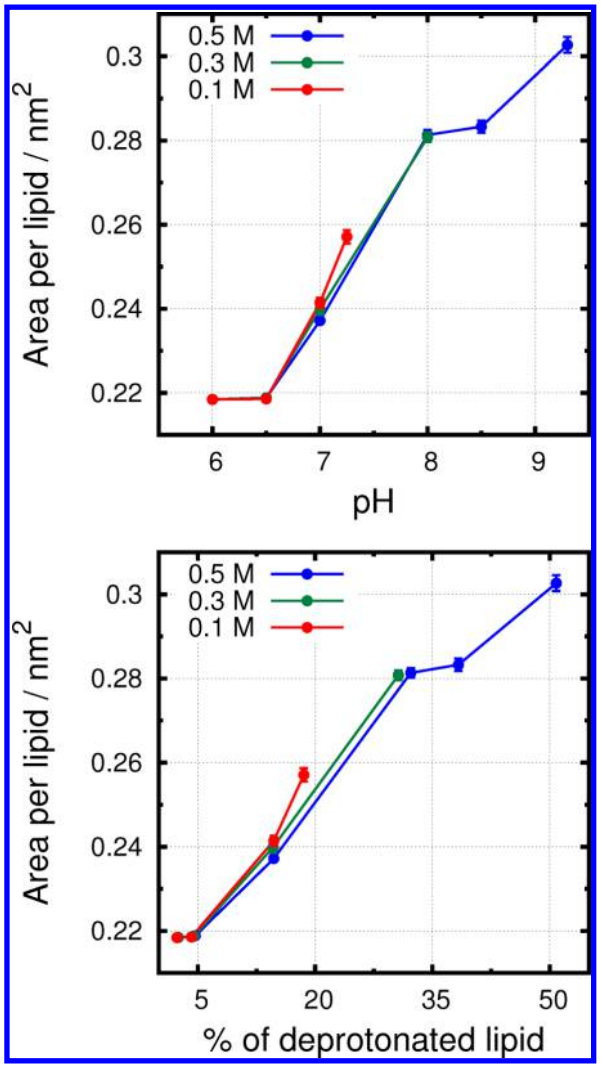

Figure 5. Average area per lipid (A_l) at different pH (upper panel) and membrane ionization (lower panel) values.

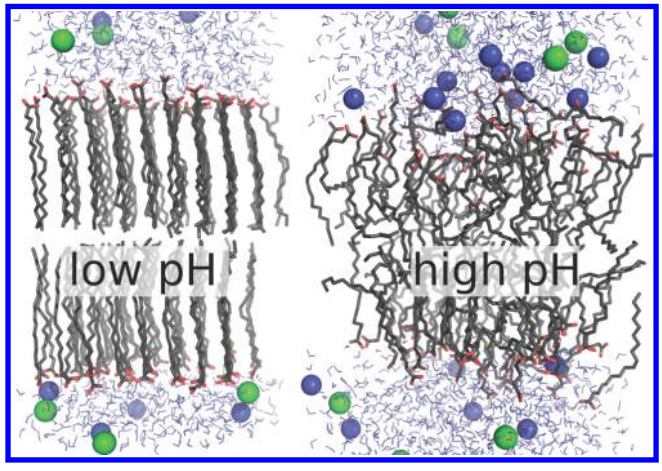

Figure 6. Graphical representation of representative configurations of our system at low and high pH values. Oleic acid molecules are shown in gray (C atoms) and red (oxygen atoms) sticks, water molecules in blue, and Cl^- and Na^+ ions in, respectively, green and blue spheres.

The isothermal phase transition can also be followed using deuterium order parameters of the oleic acid aliphatic tail (Figure 7 and Figures S6–9 in Supporting Information).

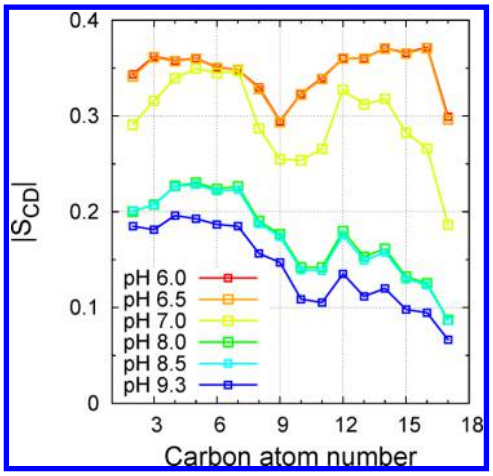

Figure 7. Deuterium order parameters for all CpHMD-L simulation at I = 0.5 M. Note that the curves for pH 6.0 and 6.5 are almost coincident, as well as those for pH 8.0 and 8.5.

Similarly to what is observed for A_l, the order of the lipidic tails changes drastically with pH/ionization. The S_{CD} values at the very ordered gel phases (0.36 for C5 at pH 6.0–6.5) are significantly higher than the available experimentally measured values for DPPC slightly below the melting temperature (0.23 for C5 at 314 K[87]). On the other hand, at higher pH values, the observed S_{CD} (0.19 for C5 at pH 9.3) are similar to the fluid phase for the oleyl chain of POPC (~0.2 for C5[88,89]). Therefore, the order parameters in our simulations also illustrate the pH-dependent isothermal phase transition already indicated by the A_l results.

Lateral diffusion of lipids is a measure of how fast the molecules diffuse along the membrane *xy* coordinates. In computer simulations, the diffusion coefficient can be obtained from the Einstein relation measuring the slope of the mean square displacement (MSD) over time. The diffusion coefficient values obtained increase with pH (Table 2 and

Table 2. Diffusion Coefficient (10^{-7} cm^2 s^{-1}) Obtained for all CpHMD-L Simulations

I/M	0.1	0.3	0.5
pH			
6.00		~0	
6.50			
7.00	1.4	0.7	0.3
7.25	4.2	–	–
8.00	–	7.3	6.1
8.50	–	–	6.6
9.30	–	–	7.8

Figures S10–12 in Supporting Information), illustrating the isothermal phase transition and an increased fluidity of the membrane. At low pH values, in the more ordered gel phase, the lipids are almost frozen in our time scale, which did not allow us to calculate their diffusion coefficient. This also helps to explain the unusually high order parameters (Figure 7), and the presence of an ionization and A_l (Figure 5) plateau observed at these pH values. At high pH values, oleic acid can diffuse approximately 1 order of magnitude faster than what has been measured for a POPC bilayer in fluid phase (0.15–0.48 × 10^{-7} cm^2 s^{-1}).[90,91]

DOI: 10.1021/acs.jctc.5b00095
J. Chem. Theory Comput. 2015, 11, 2367–2376

3.5. Counterion Concentration and Distribution near the Membrane. The total numbers of ions (n_{PB}) are estimated using a PB-based approach to determine the number of explicit ions to be placed in a MD simulation (n_{exp}). This estimation can also be performed using a Gouy−Chapman (GC)-based approach[5] (i.e., an analytical, and, hence, much faster to calculate, solution of the PB equation for an uniformly charged infinite surface). Using these two methods (PB and GC), we determined the cumulative number of counterions as a function of the distance to the membrane (Figure 8, upper panel) for a CpHMD-L simulation at pH 8.0 and I = 0.5 M. The accumulated number of explicit counterions observed in the MD simulation is also shown. The significant agreement between the MD and PB curves was expected because, in our method, their total number of ions are self-consistent. However, the number of ions estimated by the GC approach is significantly higher compared with the PB approach. This discrepancy highlights the limitations of applying a simplified approach such as GC to the irregular molecular surface of a significantly charged oleic acid bilayer with a low dielectric interior (note that the GC model lacks image-charge effects that repel the ions[92]). Apparently, the molecular detail introduced in the PB formalism is important to stabilize the strong interactions between carboxylic groups, hence, lowering the magnitude of the negative electrostatic potential near the membrane.

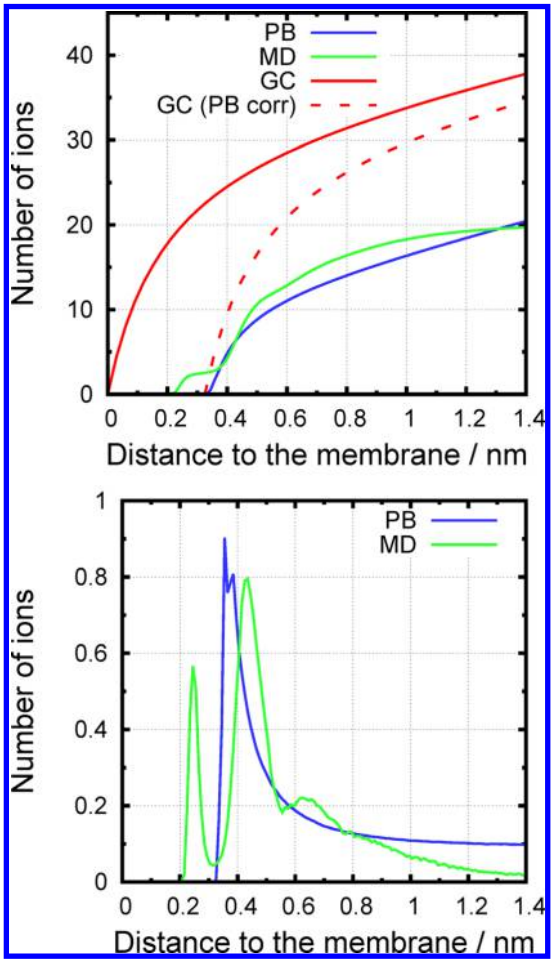

Figure 8. Variation of cumulative number (upper panel) and minimum distance histograms (lower panel) of counterions with distance to the membrane, calculated for a CpHMD-L simulation at pH 8.0 and I = 0.5 M with three different methods. The "GC (PB corr)" curve was obtained by assuming that the minimum distance of the ions to the membrane is not zero, as assumed in standard GC theory (e.g., see eq 1 in the Supporting Information of ref 5), but rather the closest distance allowed by the PB method used in this work; this corresponds to impose a Stern-like region of ion exclusion.

In our approach, the total number of explicit ions in MD is equal to the PB estimation. Nevertheless, the counter-iondistribution near the membrane can be compared (Figure 8, lower panel). The minimum distance histograms of the explicit ions show two preferential positions (around 0.25 and 0.43 nm—see Figures S13 and S14 in Supporting Information for illustrative examples), corresponding to strong interactions with the lipid headgroups. The difference between these two regions is related with the first water solvation layer of the Na^+ ions (see a radial distribution function and the number of water molecules surrounding Na^+ ions in Figures S15 and S16 in Supporting Information). At 0.43 nm, the ion is interacting with the bilayer and still retains its complete first water shell, while the strong interactions at 0.25 nm implies a partial desolvation of the ion, with the associated free energy cost. This behavior cannot be captured using a mean-field approach such as PB. Therefore, the ion distribution only shows one peak whose position (around 0.36 nm) depends only on the molecular surface and on the width of the ion exclusion layer (0.2 nm). At longer distances (between 1.0 and 1.4 nm), the MD curve diverges from PB showing an unexpected absence of ions in this region. This result is in agreement with recent results suggesting an overbinding of Na^+ ions to lipid bilayers.[93] Nevertheless, PB seems to capture the overall ion distribution profile observed in the MD simulation.

4. CONCLUSIONS

In the present work, we developed an extension to the stochastic titration constant-pH MD method[18,24] that is able to deal with PBC in x and y directions of the PB calculations and take into account the explicit ion effects at a given ionic strength value. With the PBC correction, it is possible to avoid electrostatic calculation errors that may arise from surface discontinuities at the box edges and pairwise interactions across 2D-PBC boxes.[4] Because an inadequate treatment of ionic strength effects in charged lipid bilayers may also introduce significant errors, we took advantage of a recently published PB formalism[5] to estimate the number of explicit ions in biomolecular simulations of charged bilayers to avoid such problems. As far as we know, we are presenting the first constant-pH MD simulations of continuous (infinite) lipid bilayers.

The CpHMD-L method was tested in a bilayer of oleic acid, a carboxylic acid with 18 carbons and one insaturation. With this method, we obtained titration curves that are in good agreement with the experimental data. Also, we were able to estimate the slope of the titration curve from charge fluctuations, which is a strong evidence that these are being correctly sampled in our calculations. The simulations were performed for ionizations until ∼50% because, above this value, a macroscopic transition to micelles occur. At ionic strength values below 0.5 M, we were not able to obtain a stable bilayer up to ∼50% of ionization. This observation is related with the high repulsions between charged headgroups that need to be stabilized by explicit counterions. As previously observed for a binary mixture of a zwitterionic and an anionic lipid,[5] we were able to reproduce experimental results with simulation boxes

DOI: 10.1021/acs.jctc.5b00095
J. Chem. Theory Comput. 2015, 11, 2367−2376

usually far from neutrality. This observation further supports the idea that a charged membrane strongly influences the ion distribution in its vicinity, and the neutrality is achieved significantly far from the bilayer surface.

The results obtained with this extension of the stochastic titration constant-pH MD method strongly support the importance to sample the coupling between configuration and protonation in these types of biophysical systems.[16−45] The CpHMD-L method stands now as a valuable tool to study more realistic lipid bilayers where pH can influence both lipids and solutes that might be interacting in the lipidic environment.

■ ASSOCIATED CONTENT

Supporting Information

Scheme of the CpHMD method. Time variation of A_l and membrane charge in simulations to calibrate the τ_{prt} parameter. Graphical representation of concentration of ions in all CpHMD-L simulations. Electrostatic potential mapped in membrane surface at different pH values. Order parameters at I = 0.1 M and I = 0.3 M and for the 10th methylene. Diffusion coefficient values obtained in all CpHMD-L simulations. Visualization of two typical sodium−lipid interactions. Radial distribution function and number of water molecules surrounding Na^+ ions. This material is available free of charge via the Internet at http://pubs.acs.org/.

■ AUTHOR INFORMATION

Corresponding Author

*E-mail: machuque@ciencias.ulisboa.pt. Phone:+351-21-7500112. Fax:+351-21-7500088.

Funding

We acknowledge financial support from Fundação para a Ciência e a Tecnologia through projects PTDC/QUI-BIQ/113721/2009, PTDC/QEQ-COM/1623/2012, UID/MULTI/00612/2013, and PEst-OE/EQB/LA0004/2011 and grant SFRH/BD/81017/2011.

Notes

The authors declare no competing financial interest.

■ ACKNOWLEDGMENTS

We thank Maria J. Calhorda, Sara R. R. Campos, and Hugo A. F. Santos for fruitful discussions.

■ REFERENCES

(1) Nelson, D. L., Cox, M. M. *Lehninger Principles of Biochemistry*; WH Freeman and Company: New York, 2005; pp 343−368.
(2) Kates, M.; Syz, J.-Y.; Gosser, D.; Haines, T. H. *Lipids* **1993**, *28*, 877−882.
(3) Zhou, Y.; Raphael, R. *Biophys. J.* **2007**, *92*, 2451−2462.
(4) Teixeira, V. H.; Vila-Viçosa, D.; Baptista, A. M.; Machuqueiro, M. *J. Chem. Theory Comput.* **2014**, *10*, 2176−2184.
(5) Vila-Viçosa, D.; Teixeira, V. H.; Santos, H. A. F.; Baptista, A. M.; Machuqueiro, M. *J. Chem. Theory Comput.* **2014**, *10*, 5483−5492.
(6) Hong, C.; Tieleman, P.; Wang, Y. *Langmuir* **2014**, *30*, 11993−12001.
(7) Bashford, D.; Karplus, M. *Biochemistry* **1990**, *29*, 10219−10225.
(8) Sharp, K. A.; Honig, B. *Annu. Rev. Biophys. Chem.* **1990**, *19*, 301−332.
(9) Peitzsch, R. M.; Eisenberg, M.; Sharp, K. A.; McLaughlin, S. *Biophys. J.* **1995**, *68*, 729−738.
(10) Ben-Tal, N.; Honig, B.; Peitzsch, R. M.; Denisov, G.; McLaughlin, S. *Biophys. J.* **1996**, *71*, 561−575.
(11) Ullmann, G. M.; Knapp, E.-W. *Eur. Biophys. J.* **1999**, *28*, 533−551.
(12) Teixeira, V. H.; Cunha, C. A.; Machuqueiro, M.; Oliveira, A. S. F.; Victor, B. L.; Soares, C. M.; Baptista, A. M. *J. Phys. Chem. B* **2005**, *109*, 14691−14706.
(13) Antosiewicz, J.; Porschke, D. *Biochemistry* **1989**, *28*, 10072−10078.
(14) Beroza, P.; Fredkin, D. R.; Okamura, M. Y.; Feher, G. *Proc. Natl. Acad. Sci. U.S.A.* **1991**, *88*, 5804−5808.
(15) Baptista, A. M.; Soares, C. M. *J. Phys. Chem. B* **2001**, *105*, 293−309.
(16) Mertz, J. E.; Pettitt, B. M. *Int. J. High Perform. C* **1994**, *8*, 47−53.
(17) Börjesson, U.; Hünenberger, P. *J. Chem. Phys.* **2001**, *114*, 9706−9719.
(18) Baptista, A. M.; Teixeira, V. H.; Soares, C. M. *J. Chem. Phys.* **2002**, *117*, 4184−4200.
(19) Bürgi, R.; Kollman, P.; van Gunsteren, W. *Proteins Struct. Funct. Bioinf.* **2002**, *47*, 469−480.
(20) Dlugosz, M.; Antosiewicz, J. M. *Chem. Phys.* **2004**, *302*, 161−170.
(21) Dlugosz, M., Antosiewicz, J. M., Robertson, A. D. *Phys. Rev. E* **2004***69*.
(22) Lee, M.; Salsbury, F., Jr; Brooks, C., III *Proteins Struct. Funct. Bioinf.* **2004**, *56*, 738−752.
(23) Mongan, J.; Case, D.; McCammon, J. *J. Comput. Chem.* **2004**, *25*, 2038−2048.
(24) Machuqueiro, M.; Baptista, A. M. *J. Phys. Chem. B* **2006**, *110*, 2927−2933.
(25) Machuqueiro, M.; Baptista, A. M. *Biophys. J.* **2007**, *92*, 1836−1845.
(26) Stern, H. A. *J. Chem. Phys.* **2007**, *126*, 164112.
(27) Machuqueiro, M.; Baptista, A. M. *Proteins Struct. Funct. Bioinf.* **2008**, *72*, 289−298.
(28) Campos, S. R. R.; Baptista, A. M. *J. Phys. Chem. B* **2009**, *113*, 15989−16001.
(29) Machuqueiro, M.; Baptista, A. M. *J. Am. Chem. Soc.* **2009**, *131*, 12586−12594.
(30) Campos, S. R. R.; Machuqueiro, M.; Baptista, A. M. *J. Phys. Chem. B* **2010**, *114*, 12692−12700.
(31) Itoh, S. G.; Damjanović, A.; Brooks, B. R. *Proteins Struct. Funct. Bioinf.* **2011**, *79*, 3420−3436.
(32) Machuqueiro, M.; Baptista, A. *Proteins Struct. Funct. Bioinf.* **2011**, *114*, 11659−11667.
(33) Vorobjev, Y. N. *J. Comput. Chem.* **2012**, *33*, 832−842.
(34) Swails, J. M.; Roitberg, A. E. *J. Chem. Theory Comput.* **2012**, *8*, 4393−4404.
(35) Vila-Viçosa, D.; Campos, S. R. R.; Baptista, A. M.; Machuqueiro, M. *J. Phys. Chem. B* **2012**, *116*, 8812−8821.
(36) Wallace, J. A.; Shen, J. K. *J. Chem. Phys.* **2012**, *137*, 184105.
(37) Bennett, W. F. D.; Chen, A. W.; Donnini, S.; Groenhof, G.; Tieleman, D. P. *Can. J. Chem.* **2013**, *91*, 839−846.
(38) Henriques, J.; Costa, P. J.; Calhorda, M. J.; Machuqueiro, M. *J. Phys. Chem. B* **2013**, *117*, 70−82.
(39) Carvalheda, C. A.; Campos, S. R.; Machuqueiro, M.; Baptista, A. M. *J. Chem. Inf. Model.* **2013**, *53*, 2979−2989.
(40) Chen, W.; Wallace, J. A.; Yue, Z.; Shen, J. K. *Biophys. J.* **2013**, *105*, L15−L17.
(41) Vila-Viçosa, D.; Teixeira, V. H.; Santos, H. A. F.; Machuqueiro, M. *J. Phys. Chem. B* **2013**, *117*, 7507−7517.
(42) Goh, G. B.; Hulbert, B. S.; Zhou, H.; Brooks, C. L. *Proteins Struct. Funct. Bioinf.* **2014**, *82*, 1319−1331.
(43) Lee, J.; Miller, B. T.; Damjanovic, A.; Brooks, B. R. *J. Chem. Theory Comput.* **2014**, *10*, 2738−2750.
(44) Swails, J. M.; York, D. M.; Roitberg, A. E. *J. Chem. Theory Comput.* **2014**, *10*, 1341−1352.
(45) Vila-Viçosa, D.; Francesconi, O.; Machuqueiro, M. *Beilstein J. Org. Chem.* **2014**, *10*, 1513−1523.
(46) Khandogin, J.; Brooks, C. L. *Biophys. J.* **2005**, *89*, 141−157.
(47) Khandogin, J.; Brooks, C. L. *Biochemistry* **2006**, *45*, 9363−9373.
(48) Donnini, S.; Tegeler, F.; Groenhof, G.; Grubmüller, H. *J. Chem. Theory Comput.* **2011**, *7*, 1962−1978.

DOI: 10.1021/acs.jctc.5b00095
J. Chem. Theory Comput. 2015, 11, 2367−2376

(49) Kong, X.; Brooks, C. L., III *J. Chem. Phys.* **1996**, *105*, 2414−2423.
(50) Morrow, B.; Koenig, P.; Shen, J. *J. Chem. Phys.* **2012**, *137*, 194902−194902.
(51) Torrie, G. M.; Valleau, J. P. *Chem. Phys. Lipids* **1979**, *65*, 343−346.
(52) Jönsson, B.; Wennerstroem, H.; Halle, B. *J. Phys. Chem.* **1980**, *84*, 2179−2185.
(53) Lakhdar-Ghazal, F.; Tichadou, J.-L.; Tocanne, J.-F. *Eur. J. Biochem.* **1983**, *134*, 531−537.
(54) Guldbrand, L.; Jönsson, B.; Wennerström, H.; Linse, P. *J. Chem. Phys.* **1984**, *80*, 2221−2228.
(55) Andelman, D. In *Handbook of biological physics*; Lipowsky, R., Sackmann, E.; Elsevier Science: Washington, DC, 1995; Vol. *1*, pp 603−642.
(56) Smart, J. L.; McCammon, J. A. *J. Am. Chem. Soc.* **1996**, *118*, 2283−2284.
(57) Mengistu, D. H.; Kooijman, E. E.; May, S. *Biochem. Biophys. Acta, Biomembr.* **2011**, *1808*, 1985−1992.
(58) Israelachvili, J. N. *Intermolecular and Surface Forces: Revised*, 3rd ed.; Academic Press: San Diego, 2011; pp 291−340.
(59) Haines, T. *Proc. Natl. Acad. Sci. U.S.A.* **1983**, *80*, 160.
(60) Cistola, D. P.; Hamilton, J. A.; Jackson, D.; Small, D. M. *Biochemistry* **1988**, *27*, 1881−1888.
(61) Salentinig, S.; Sagalowicz, L.; Glatter, O. *Langmuir* **2010**, *26*, 11670−11679.
(62) Peterlin, P.; Arrigler, V.; Kogej, K.; Svetina, S.; Walde, P. *Chem. Phys. Lipids* **2009**, *159*, 67−76.
(63) Janke, J. J.; Bennett, W. F. D.; Tieleman, D. P. *Langmuir* **2014**, *30*, 10661−10667.
(64) Small, D. M.; Cabral, D. J.; Cistola, D. P.; Parks, J. S.; Hamilton, J. A. *Hepatology* **1984**, *4*, 77S−79S.
(65) Kanicky, J. R.; Shah, D. O. *J. Colloid Interface Sci.* **2002**, *256*, 201−207.
(66) Tanford, C. *Physical Chemistry of Macromolecules*; John Wiley & Sons, Inc.: New York, 1961; pp 572−573.
(67) Wyman, J. *Binding and Linkage: Functional Chemistry of Biological Macromolecules*; University Science Books: Herndon, VA, 1990; p 75.
(68) Chandler, D. *Introduction to Modern Statistical Mechanics*; Oxford University Press: New York, 1987; p 71.
(69) Knott, G. D. *Interpolating Cubic Splines*; Birkhäuser: Boston, 1999; p 71.
(70) Schmid, N.; Eichenberger, A.; Choutko, A.; Riniker, S.; Winger, M.; Mark, A.; Van Gunsteren, W. *Eur. Biophys. J.* **2011**, *40*, 843−856.
(71) van der Spoel, D.; Lindahl, E.; Hess, B.; Groenhof, G.; Mark, A. E.; Berendsen, H. J. C. *J. Comput. Chem.* **2005**, *26*, 1701−1718.
(72) Hess, B.; Kutzner, C.; Van Der Spoel, D.; Lindahl, E. *J. Chem. Theory Comput.* **2008**, *4*, 435−447.
(73) Poger, D.; Mark, A. E. *J. Chem. Theory Comput.* **2010**, *6*, 325−336.
(74) Hermans, J.; Berendsen, H. J. C.; van Gunsteren, W. F.; Postma, J. P. M. *Biopolymers* **1984**, *23*, 1513−1518.
(75) Hess, B. *J. Chem. Theory Comput.* **2008**, *4*, 116−122.
(76) Miyamoto, S.; Kollman, P. *J. Comput. Chem.* **1992**, *13*, 952−962.
(77) Bussi, G.; Donadio, D.; Parrinello, M. *J. Chem. Phys.* **2007**, *126*, 014101.
(78) Berendsen, H. J. C.; Postma, J. P. M.; van Gunsteren, W. F.; DiNola, A.; Haak, J. R. *J. Chem. Phys.* **1984**, *81*, 3684−3690.
(79) Tironi, I. G.; Sperb, R.; Smith, P. E.; van Gunsteren, W. F. *J. Chem. Phys.* **1995**, *102*, 5451−5459.
(80) Smith, P. E.; van Gunsteren, W. F. *J. Chem. Phys.* **1994**, *100*, 3169−3174.
(81) Rocchia, W.; Sridharan, S.; Nicholls, A.; Alexov, E.; Chiabrera, A.; Honig, B. *J. Comput. Chem.* **2002**, *23*, 128−137.
(82) Li, L.; Li, C.; Sarkar, S.; Zhang, J.; Witham, S.; Zhang, Z.; Wang, L.; Smith, N.; Petukh, M.; Alexov, E. *BMC Biophys.* **2012**, *5*, 9.
(83) Gilson, M.; Sharp, K.; Honig, B. *J. Comput. Chem.* **1987**, *9*, 327−335.
(84) Dippy, J. F. J.; Hughes, S. R. C.; Rozanski, A. *J. Chem. Soc.* **1959**, 2492−2498.
(85) Neale, C. Note: GROMACS Bug # 1166: g_order is incorrect for unsaturated carbons. http://redmine.gromacs.org/issues/1166 (accessed September 15, 2014).
(86) Allen, M. P., Tildesley, D. J. *Computer Simulation of Liquids*; Oxford University Press: New York, 1987; pp 191−198.
(87) Seelig, A.; Seelig, J. *Biochemistry* **1974**, *13*, 4839−4845.
(88) Seelig, J.; Waespe-Sarcevic, N. *Biochemistry* **1978**, *17*, 3310−3315.
(89) Perly, B.; Smith, I. C. P.; Jarrell, H. C. *Biochemistry* **1985**, *24*, 1055−1063.
(90) Guo, L.; Har, J. Y.; Sankaran, J.; Hong, Y.; Kannan, B.; Wohland, T. *ChemPhysChem* **2008**, *9*, 721−728.
(91) Macháň, R.; Hof, M. *Biochem. Biophys. Acta, Biomembr.* **2010**, *1798*, 1377−1391.
(92) Jackson, J. D. *Classical Electrodynamics*; John Wiley and Sons, Inc.: New York, 1999; pp 154−157.
(93) Venable, R. M.; Luo, Y.; Gawrisch, K.; Roux, B.; Pastor, R. W. *J. Phys. Chem. B* **2013**, *117*, 10183−10192.

DOI: 10.1021/acs.jctc.5b00095
J. Chem. Theory Comput. 2015, 11, 2367−2376